Memoirs of the Faculty of Engineering, Okayama University, Vol.29, No. 2, pp. 5 -12, March 1995

Numerical Study on Transient Heat Characteristics of a Rectangular Latent Heat Storage Vessel

Hideo INABA*, Ping TU** and Koichi OZAKI*

(Received January 27 , 1995)

Transient characteristics of the rectangular latent heat storage vessel packed with shape-stabilized phase change (solid-liquid) material (PCM) are investigated numerically by solving the governing equations of both the PCM and the heat transfer medium(water) simultaneously as a conjugate problem with the finite difference technique. It's found that the heat storage characteristics are greatly affected by the flow direction of the heat transfer medium since the natural and forced convection coexists in the heat storage vessel. That is, it is classified that the effectively thermal efficiency of the latent heat storage system is obtained by the downflow along vertical PCM for heat storage process and the upflow for heat release process. The effect of the inlet velocity of heat transfer medium(water) on transient heat characteristics of the latent heat storage system is also revealed in the present study.

1 INTRODUCTION

The latent heat storage systems are widely utilized to consume energy efficiently and economically. As a specific application, using the off-peak electric power during the midnight, the heat can be stored into the latent heat storage material economically. The stored energy is used during the day time avoiding the period of the peak electric power demands. Therefore, for this type of heat storage system, the shorter time that the heat storage process takes and the higher output temperature of the heat transfer medium during the heat release process should be desirable. A new type of PCM[1] that consists of the shape-stabilized paraffin dispersed within the polyethylene as the basic material is utilized in the present heat storage system. It is an attractive heat storage material which keeps its shape even if the paraffin as the PCM melts completely, since the PCM can contact with the heat transfer fluid directly without the heat resistence.

The rectangular heat storage vessel is composed of a number of rectangular cross-sectioned channels for the heat transfer medium arranged in paralled and separated by the PCM as shown in Fig.1. As the arrangement of all the channels and heat storage section is identical and the each heat transfer medium flow rate in the channels is equal, the analysis can thus be restricted to the consideration of a section composed of only one-half of the channel and the PCM as shown in Fig.2. When the inlet velocity of the heat transfer medium is in the direction of the gravity, the calculating model is called the downflow model. Otherwise, it is called the upflow model.

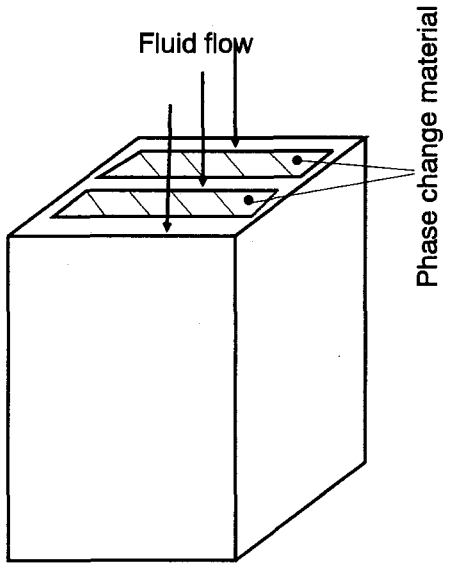

Fig.1 The schematic of the heat storage unit

* Department of Mechenical Engineering
** Graduate School of Okayama University

2 NOMENCLATURE

c: specific heat
c_{pe}: equivalent apparent heat capacity
L: length of the heat storage unit
P: pressure
T: temperature
T_{out}: outlet bulk temperature
U, V: velocity
W1: half width of PCM
W2: half width of the flowing channel
x, y: coordinate directions
Greek Symbols
ρ: density
τ: time
μ: dynamic viscosity
λ: thermal conductivity
β: volume expansion coefficient at constant pressure
Subscripts
0: initial condition
in: inlet
out: outlet

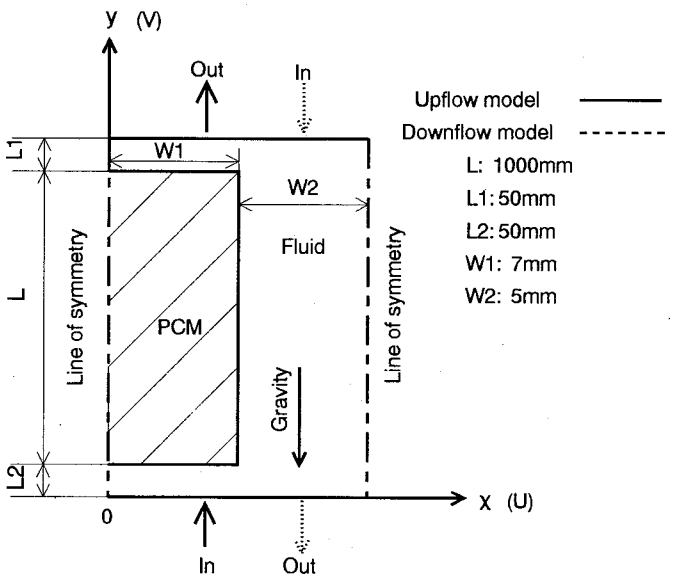

Fig.2 The analysing model(cross section of the heat storage unit,not scale)

3 MATHEMATICAL MODELING

The continuity, momentum, and energy conserving equations of two-dimensional transient incompressible laminar flows are as follows:

- continuity equation

$$\frac{\partial u}{\partial x}+\frac{\partial v}{\partial y}=0 \tag{1}$$

- momentum equations

$$\frac{\partial u}{\partial t}+u\frac{\partial u}{\partial x}+v\frac{\partial u}{\partial y} = \nu\left(\frac{\partial^2 u}{\partial x^2}+\frac{\partial^2 u}{\partial y^2}\right)-\frac{1}{\rho}\frac{\partial P}{\partial x} \tag{2}$$

$$\frac{\partial v}{\partial t}+u\frac{\partial v}{\partial x}+v\frac{\partial v}{\partial y} = div(\nu\, grad\, V)-\frac{1}{\rho}\frac{\partial P}{\partial y}-g \tag{3}$$

- energy equation

$$\frac{\partial(\rho c_{pe}T)}{\partial t}+u\frac{\partial(\rho c_{pe}T)}{\partial x}+v\frac{\partial(\rho c_{pe}T)}{\partial y}=div(\lambda\, grad\, T) \tag{4}$$

In equation(3), Boussinesq approximation is applied, that is

$$\rho^*=\rho_c\{1-\beta(T-T_c)\}$$

For the PCM, the c in the energy equation is written as c_{pe}, and the c_{pe} is the equivalent apparent heat capacity. If there is no phase change, the c_{pe} is equil to the apparent heat capacity. When the phase changes, the c_{pe} includes both of apparent heat and latent heat of the PCM, and the relationship between c_{pe} and temperature is derived from the measured results of the shape-stabilized PCM by using DSC[1].

The initial and boundary conditions for the case of uniform inlet conditions are defined as follows:

- initial condition

$$t=0 \;:\; u=v=0 \;,\; T=T_0 \tag{5}$$

- boundary condition for velocity

$$\begin{cases} x = 0\text{mm} & : \dfrac{\partial v}{\partial x} = 0 \ , \ u = 0 \\ y = 0\text{mm} & : v = v_{in} \ , \ u = 0 \\ x = 12\text{mm} & : \dfrac{\partial v}{\partial x} = 0 \ , \ u = 0 \end{cases} \tag{6}$$

- boundary condition for temperature

$$\begin{cases} x = 0\text{mm} & : \dfrac{\partial T}{\partial x} = 0 \\ y = 0\text{mm} & : T = Tin \\ x = 12\text{mm} & : \dfrac{\partial T}{\partial x} = 0 \end{cases} \tag{7}$$

4 NUMERICAL PROCEDURE

The solution procedure used for solving the above equations is the control-volume finite-difference approach described by Patankar[2]. In this methodology, the domain is discretised into a number of control volumes (each associated with a nodal point)such that some control volume faces coincide with the PCM-heat transfer medium(water)interface. The pressure-velocity interlinkage is handled by using SIMPLE scheme[2]. The converged results for velocity and pressure are assumed to be reached on these conditions that are the sum of the residuals of the continuity equation is less than 10^{-8} and the maximum of the residuals is less than 10^{-5} . Furthermore, the iteration for temperature is continued until the sum of the residuals of energy conserving equations is less than 10^{-4} and the maximum relative change of temperature between consecutive iterations is less than 10^{-4} . For every time step, the calculation is also checked by observing the energy balance in the whole solution domain. Results show the sum of the heat released from(or the heat stored in) the PCM, and the heat transfer medium(water) is eaual to the whole enthalpy difference between the inlet and outlet heat transfer medium within the range of $\pm 0.1\%$

5 NUMERICAL RESULTS AND DISCUSSION

The geometrical variables keep at constant values of $L = 1m, W1 = 7mm, and\ W2 = 5mm$ in the present analysis. The PCM and the heat transfer medium(water) are initially static and at the same initial temperature T_0 . At the entrance in width of $(W1 + W2)$, the heat transfer medium has a uniform temperature distribution (T_{in}) and uniform velocity distribution (V_{in}) .

5.1 Comparison of the Numerical Results with the Experimental Ones

At first the above equations and numerical procedures were checked against experimental results . As shown in Fig.3 , in the heat storage process, the heat transfer medium flows down as shown in Fig.2. Comparing the calculated outlet bulk temperature T_{out} of the heat transfer medium with that measured, it can be seen that the present numerical result agrees well with the experimental one.

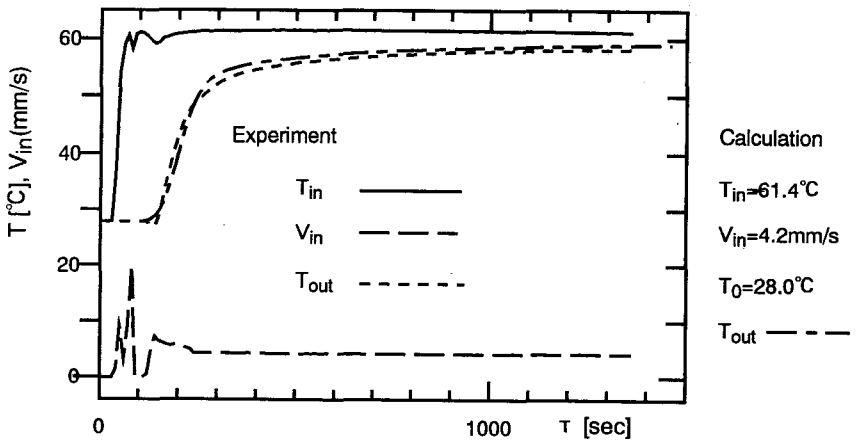

Fig.3 Comparison of the numerical result with experimental one

In order to investigate the effect of flowing direction for the heat storage and heat release processes, the numerical computations of both upflow and downflow model for different process are conducted.

5.2 Heat Storage Characteristics

For the heat storage process, when the inlet velocity V_{in} , the inlet temperature T_{in} and the initial temperature of the rectangular heat storage vessel T_0 equal $1.6mm/sec, 60\ ℃, 45\ ℃$ respectively, the numerical results of upflow model are given in Figs.4 and 5. Under the same calculating conditions, the numerical results of downflow model are shown in Figs.6 and 7. As shown in Fig.4, the temperature of the heat transfer medium close to the PCM ($x = W1$) is lower than that of near the centerline ($x = W1+W2$). Therefore the density of the heat storage medium near the PCM is larger. As a result, natural convection occurs and causes the heat transfer medium near the PCM to flow against the upflow of forced convection. On the other hand, for downflow model, as shown in Fig.6, the velocity profile has a quite different shape against that in Fig.4 , and the heat transfer medium near the PCM is accelerated by the natural convection near the PCM. Therefore, the heat transfer between the PCM and the fluid is enhanced in this case, contrasting to the upflow model. Comparing the melting fronts between Fig.5 and Fig.7 at different times, the melting fronts for downflow model moves faster than that of upflow model due to ascending flow near the PCM by natural convection. It can be seen that the downflow can meet the demand of shortening the heat storage period.

5.3 Heat Release Characteristics

For the heat release process, when the inlet velocity V_{in} , the inlet temperature T_{in} and the initial temperature of the rectangular heat storage vessel T_0 are equal to $1.1mm/sec, 45\ ℃, 60\ ℃$, respectively. The numerical results of upflow model are given in Figs.8 and 9 . Under the same initial and boundary conditions, the numerical results of downflow model are given in Figs.10 and 11. The temperature of the heat transfer medium(water) near the PCM is higher and its density is smaller than those of the heat transfer medium close to the centerline ($x = W1 + W2$) . As indicated in Fig.10, the heat transfer medium near PCM changes its flowing direction, and the heat transfer medium close to the centerline is accelerated considerably as the total mass flow is fixed. Therefore the output bulk temperature T_{out} falls down immediately after the heat release process begins. Because for the specific application in which the high output bulk temperature is desirable, the above case should be avoided and the upflow model is favorable as in this case the output bulk temperature T_{out} can keep relatively higher value for a long time as shown in Fig.12.

The inlet velocity of the heat transfer medium is also an important factor to know the characteristics of the rectangular heat storage vessel besides of flowing direction. The effects of inlet velocity are illustrated in Figs.13, 14 and 15. The τ_f is the finishing time of the heat storage process or heat release process. Fig.13 shows that for the heat storage process and downflow model, the larger the inlet velocity of heat storage medium, the shorter the heat storage time. On the other hand, for heat release process and upflow model, as shown in Figs.14 and 15, as the inlet velocity of the heat transfer medium decreases, the time to finish the whole process increases and higher output bulk temperature can be gained.

6 CONCLUSION

A rectangular heat storage vessel with the configuration in Fig.1 has been studied numerically. The obtained results show that the flowing direction and inlet velocity of heat transfer medium influence its transient characteristics significantly. In order to meet the demand of the specific application, downflowing and larger inlet velovity of the heat transfer medium is satisfied for heat storage process, and for heat release process, upflowing and smaller inlet velocity is suitable. This conclusion provides guidelines for the design of the heat storage unit. More extensive parametric investigation is due to be continued.

References

[1] H.Inaba et al., 15th Jap. Symposium on Thermophysical Properties, (1994) ,pp.211-214.

[2] S. V. Patankar , Numerical Heat Transfer and Fluid Flow, McGraw-Hill, New York (1980).

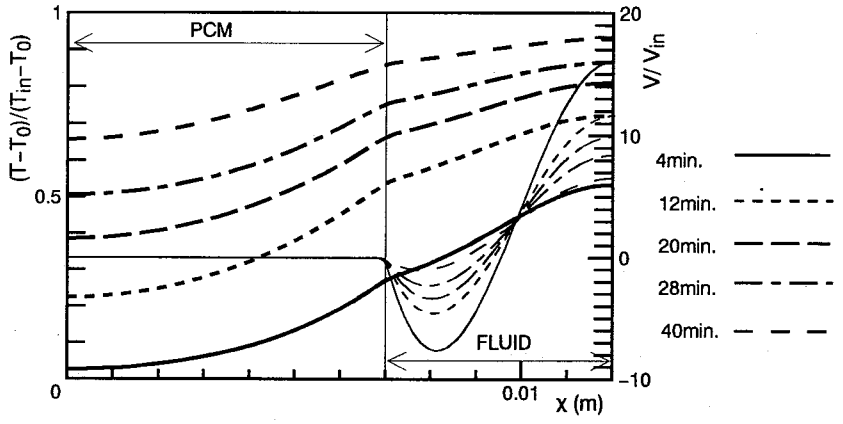

Fig.4 Temperature distribution and streamwise velocity distribution at y=550mm

(the thick line: temperature; the thin line: velocity;heat storage process,upflowing)

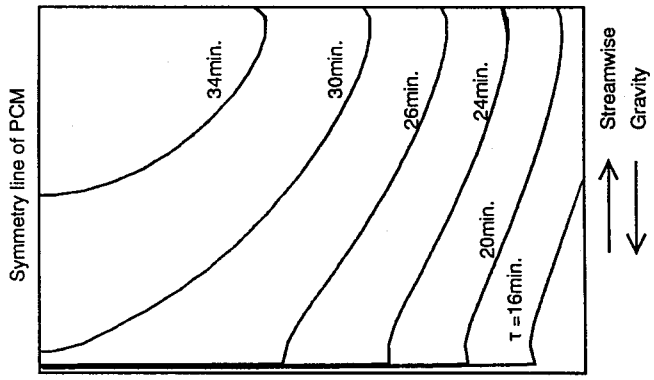

Fig.5 PCM's melting fronts with time τ

(heat storage process, upflowing)

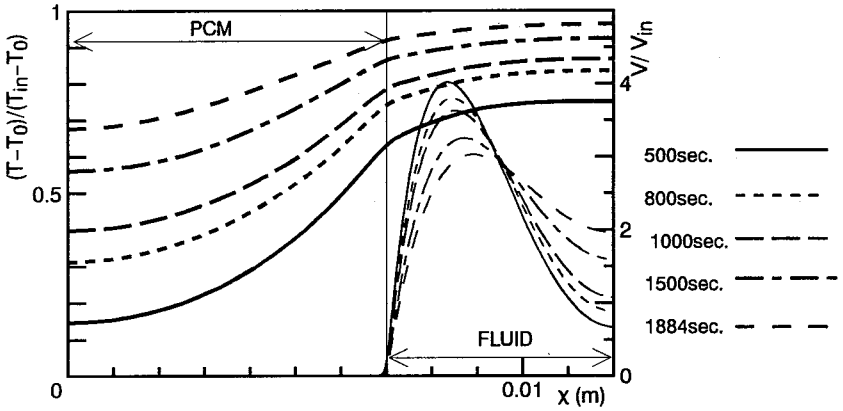

Fig.6 Temperature distribution and streamwise velocity distribution at y=550mm

(the thick line: temperature; the thin line: velocity; heat storage process, downflowing)

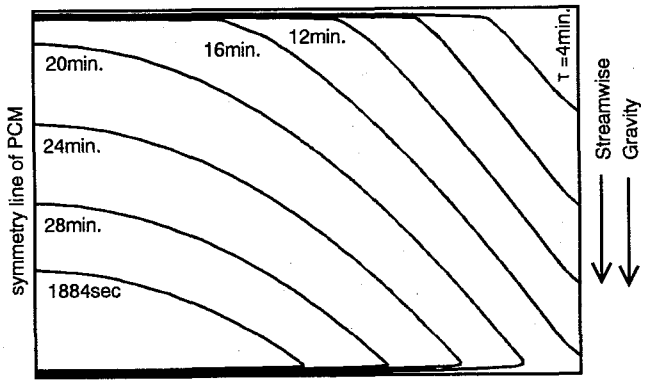

Fig.7 PCM's Freezing fronts with time τ
(heat storage process, downflowing)

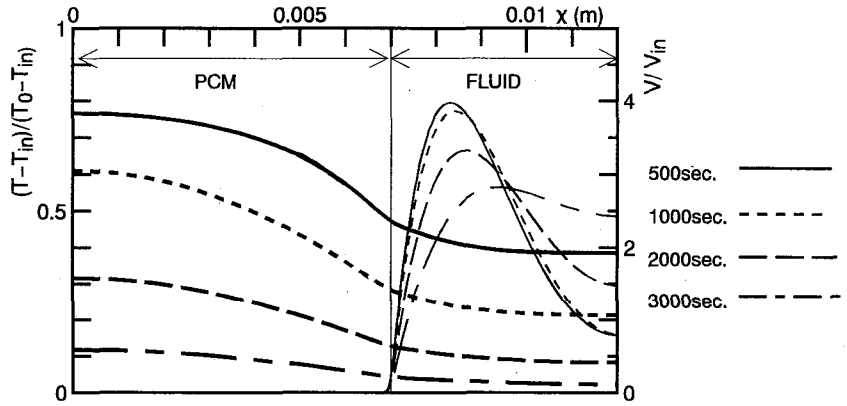

Fig.8 Temperature distribution and streamwise velocity distribution at y=550mm
(the thick line: temperature; the thin line: velocity; heat release process, upflowing)

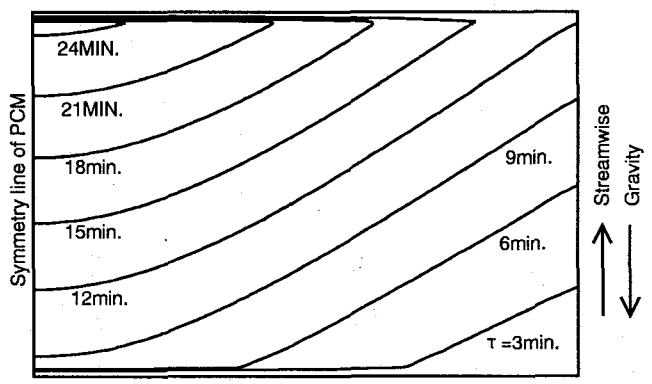

Fig.9 PCM's freezing fronts with time τ
(heat resease process, upflowing)

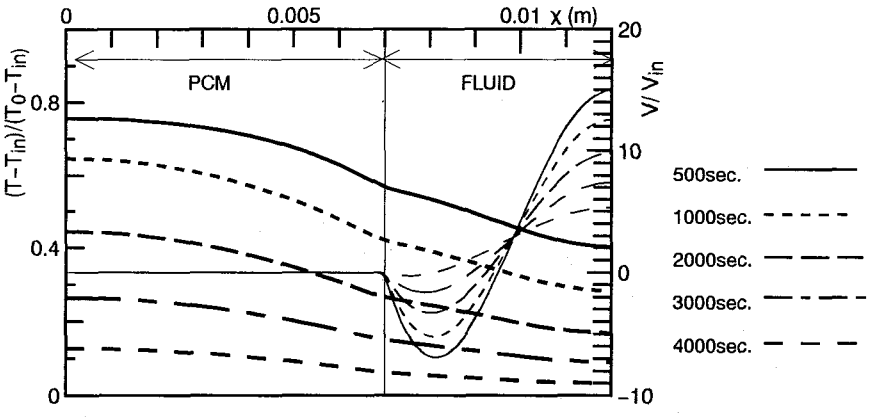

Fig.10 Temperature distribution and streamwise velocity distribution at y=550mm

(the thick line: temperature; the thin line: velocity; heat release process, downflowing)

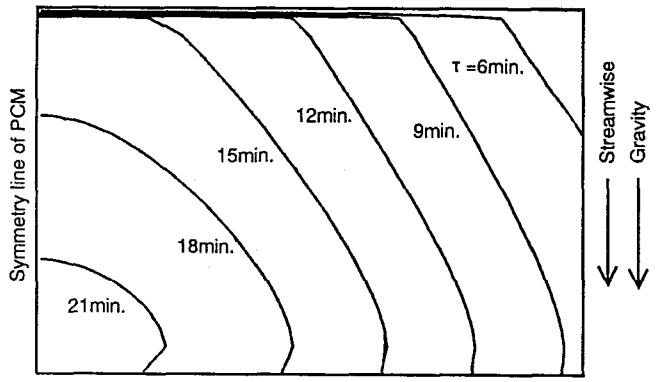

Fig.11 Freezing fronts for various time periods

(heat release process, downflowing)

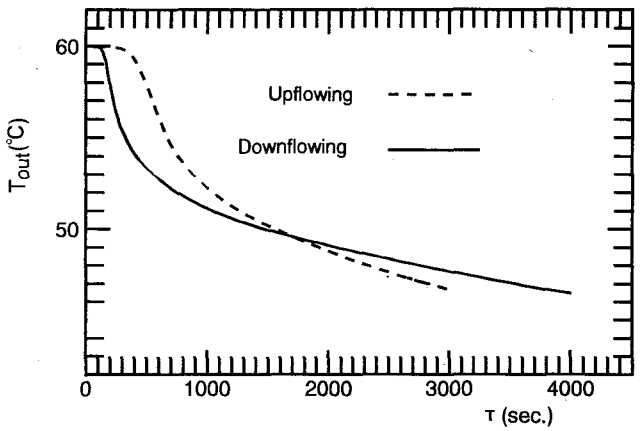

Fig.12 The outlet bulk temperature for different flowing direction

(heat resease process)

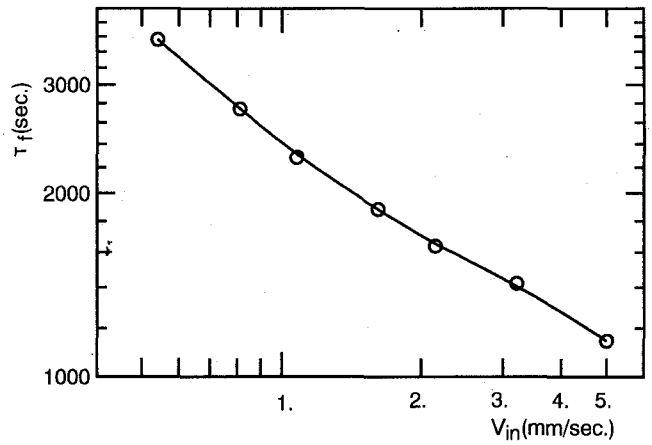

Fig.13 The variation finishing times with inlet velocity
(heat storage process,downflowing)

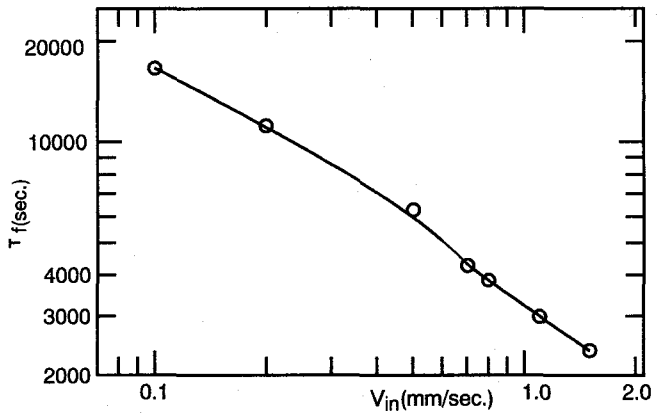

Fig.14 The finishing time for various inlet velocities
(heat release process, upflowing)

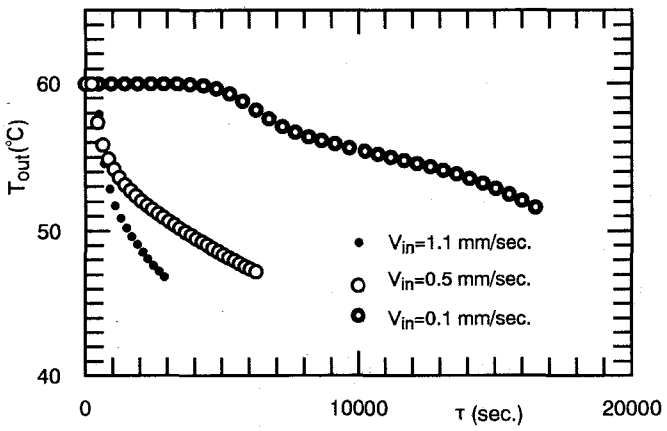

Fig.15 The outlet bulk temperature for various inlet velocities
(heat release process, upflowing)